C20

4D Geoelectrical Monitoring of Natural Attenuation Processes at a Contaminated Former Gas-works Site

P.B. Wilkinson* (British Geological Survey), P.I. Meldrum (British Geological Survey), O. Kuras (British Geological Survey), J.E. Chambers (British Geological Survey), S.J. Holyoake (British Geological Survey) & R. D. Ogilvy (British Geological Survey)

SUMMARY

A permanent automated geoelectrical imaging system was installed at a contaminated land site to monitor resistivity changes associated with groundwater quality after the completion of a remediation programme. The former gasworks site had been designated statutory contaminated land due to the risks of pollution of an underlying minor aquifer. The system collected data at regular scheduled intervals from a network of electrodes arranged in vertical borehole arrays on the boundaries of the site. The incoming data from the system were automatically inverted to produce 4D resistivity images. Analysis was carried out over one year, revealing resistivity fluctuations in the infilled ground beneath the tarmac that were strongly temperature dependent. But in the underlying sand and gravel aquifer there was a steady increase in resistivity that was suggestive of a reduction in groundwater contamination after the removal of the contaminant source zones. A tracer test was also undertaken to investigate the groundwater flow velocity and demonstrate rapid 4D geoelectrical monitoring of natural attenuation processes. The motion and evolution of the tracer were visualised directly in high-resolution volumetric images in near realtime. Seepage velocities measured from the images agreed closely with estimates based on the piezometric gradient and assumed material parameters.

Introduction

Assessing the effectiveness of remediation techniques with certainty can be difficult and time-consuming, since traditional intrusive sampling can only test statistically small volumes of ground. But because the geoelectrical properties of earth materials are sensitive to the presence of contaminants and their break-down products, time-lapse geoelectrical imaging can act as a surrogate monitoring technology for tracking and visualising changes in contaminant concentrations. This minimally-invasive 4D volumetric monitoring technique has the potential to complement, and reduce the need for, intrusive point sampling.

Test site description

A permanent geoelectrical subsurface imaging system was installed at a contaminated land test site, the Wharf Road municipal car-park in Stamford, Lincolnshire. The site had been constructed on a former gas-works and had been polluted by a range of polyaromatic hydrocarbons and dissolved phase contaminants. It was designated statutory contaminated land under Part IIA of the Environmental Protection Act due to the risk of polluting an underlying minor aquifer. The aim of the installation was to monitor changes in groundwater quality after the completion of a remediation programme, which consisted of excavation and removal of highly contaminated materials, and ex-situ bioremediation of other soils. The system was based on BGS-designed ALERT technology and comprised an automated geoelectrical imaging instrument, wireless internet communication link, batteries and mains charging. It collected resistivity data according to a programmable schedule from 224 subsurface electrodes arranged at 0.5 m depth intervals in 14 vertical arrays, with each array extending to a depth of 8 m below ground level (bgl) (Figure 1). The arrays were arranged to monitor two boundaries of the site, bordering the River Welland to the south and privately owned land to the east. They were installed during the remediation works using a sonic drilling method in full compliance with Environment Agency and Health & Safety Executive regulatory requirements. Several groundwater monitoring boreholes were also installed, which provided intrusive geochemical sampling data with which to calibrate the resistivity monitoring images.

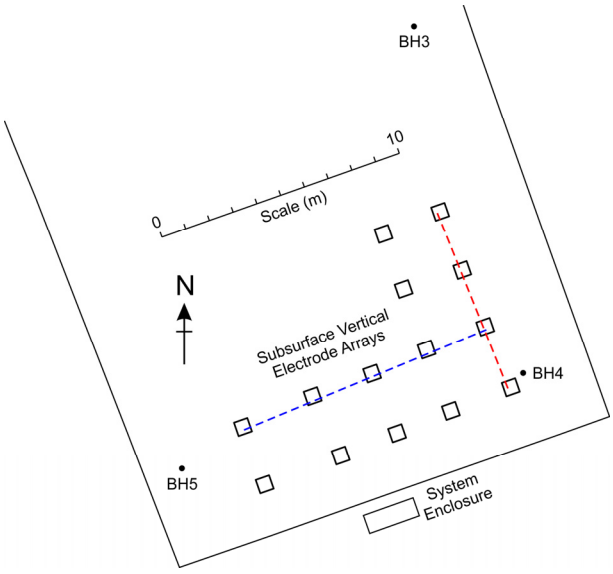

Figure 1. Scale diagram of the monitoring region showing the locations of the electrode arrays, groundwater monitoring boreholes and system enclosure. Dashed lines show locations of resistivity model slices (Figure 2).

A subsurface resistivity image obtained in September 2008 during post-remediation monitoring is shown in Figures 2a & b. The data were inverted with the Res3DInv software using a finite difference method, the incomplete Gauss-Newton solver, an L_1-norm data constraint, and an L_2-norm model constraint weighted by a factor of 2 to emphasize horizontal structure. Figure 2a shows a vertical slice through the 3D resistivity model from west to east along the blue dashed line in Figure 1. Similarly Figure 2b shows a vertical slice from south to north along the red dashed line. After 10 iterations, the mean misfit error between the modelled and observed resistivity data had converged to ~3%. A lithological log obtained during the installation of the arrays is shown to the right of the resistivity images at the same depth scale. The top 3 m of bioremediated, infilled ground are predominantly resistive, since

they are less well compacted than the undisturbed ground beneath and are therefore better drained. The Flandrian river alluvium, at depths of ~3-5 m bgl, is very conductive due to its high clay content. Beneath this, at depths of ~5-6 m bgl, is the minor aquifer consisting predominantly of sands and gravel. Electrical conduction in this layer is dominated by the groundwater, which is more resistive than the clay-rich alluvium. The log then indicates further sands and gravels, above the Whitby Mudstone at depths of more than 7 m bgl. The images exhibit thin alternating resistive and conductive layers, possibly underlain by conductive bedrock at ~8 m bgl. Two of these three resistive layers do not appear to be continuous, although their disappearance with increasing distance from the borehole electrodes is probably due to the associated decrease in image resolution with increasing distance (Oldenborger *et al.*, 2007). It is possible that the lack of quantitative agreement between the logs and the images below 6 m bgl is due to slippage in the core barrel, which has previously been observed when using the sonic drilling method (Wilkinson *et al.*, 2008).

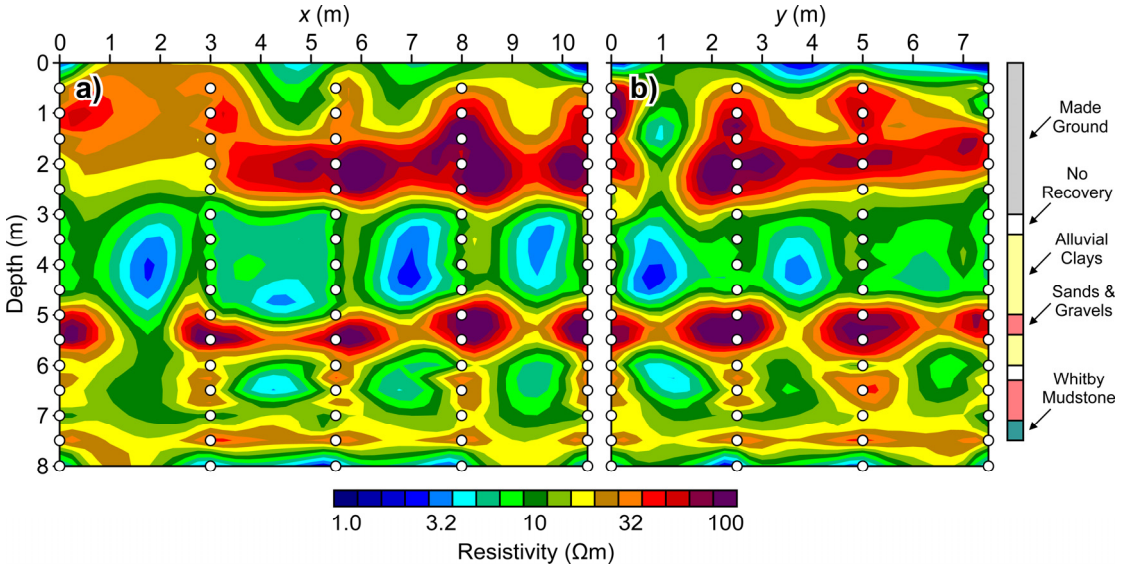

Figure 2. 2D slices through the 3D resistivity image along a) blue and b) red dashed lines in Figure 1. White circles indicate electrode locations. A lithological log is shown on the right.

Monitoring

The primary aim of the project was to monitor changes in the subsurface resistivity associated with the remediation process. The changes that occurred during a year-long monitoring period were subtle, and are displayed in Figure 3 as average resistivities in the infilled ground (0-3 m bgl), the minor aquifer (5-6 m bgl) and the deeper river terrace deposits (7-7.5 m bgl). There are strong correlations between the average resistivity of the infilled ground and the air temperature averaged over the week preceding the measurement (black dashed line in Figure 3, measured at RAF Wittering, 3 miles to the SSE). This is to be expected, since the black tarmac covering the infilled ground will couple it efficiently to solar heating, which in turn will affect the resistivity near the surface. Until early July 2008, the resistivity and air-temperature are anti-correlated, which is similar to the behaviour of Arps' empirical formula (Arps, 1953) describing how the resistivities of formation waters decrease with increasing temperature. After this, the effect switches abruptly to a positive correlation, in which increased temperatures (in this case, above ~15°C) lead to increased resistivities. The reason for this abrupt change in correlation is not clear.

It is known that temperature changes due to heating at the surface decrease exponentially with increasing depth, and also exhibit an increasing time lag. This is typically of the order of a few hours above 1 m bgl, rising to many weeks at 3 m bgl. In the deeper river terrace deposits, the resistivity is very stable (red line), changing by < 5% over the year. The removal

of the contaminant source zones in the made ground has had little effect on the groundwater in this layer, which is reasonable since there are two intervening layers of clay and alluvium.

By contrast, the minor aquifer exhibited a steady increase in resistivity (purple line) until mid-March 2008, beyond which it remains approximately constant. There is little evidence of any seasonal changes due to either infiltration or temperature. This is also to be expected, since the site is covered by an impermeable tarmac layer, and the exponential decrease of temperature changes with depth suggests that any temperature-induced effects would be only ~2.5% of the magnitude of those in the infilled ground. Therefore it seems reasonable to conclude that the increase in resistivity is likely to be due to an improvement in the quality of groundwater, i.e. a decrease in dissolved compounds. Groundwater samples were taken bi-monthly, but the data were highly variable with no obvious trends over time for any of the tested contaminants in any of the monitoring boreholes. It was not possible, therefore, to use the groundwater data either to confirm or refute the hypothesis that the increase and subsequent plateau in the resistivity of the minor aquifer was due to improved groundwater quality.

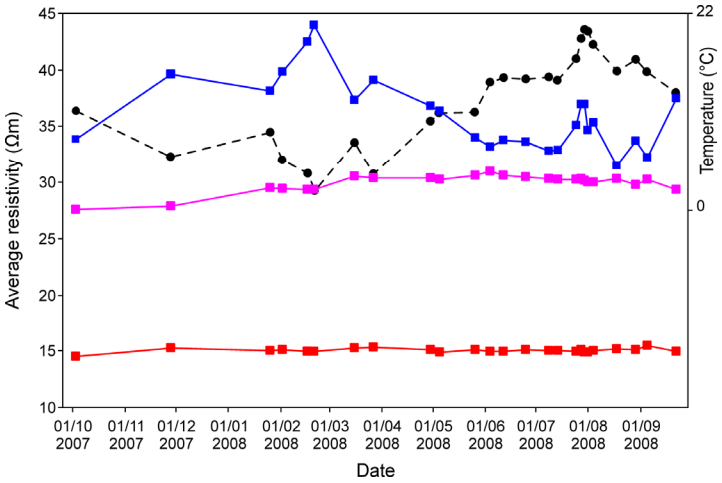

Figure 3. Average resistivity of the infilled ground (blue), minor aquifer (purple), and the deeper gravel layer (red). The weekly averaged air temperature is also shown (dashed black). Temperature data provided by UK Meteorological Office. MIDAS Land Surface Stations data (1853-current), [Internet]. British Atmospheric Data Centre, 2006, Apr 2009. Available from http://badc.nerc.ac.uk/data/ukmo-midas.

Tracer Test

To investigate the groundwater flow direction and speed, and also to provide a clear demonstration of the capabilities of 4D geoelectrical contamination and remediation monitoring, a tracer test was undertaken in which a conductive tracer was introduced into one of the groundwater monitoring boreholes, and its dispersion and dilution monitored in near real-time. Piezometric levels were measured directly in BH3-5 to determine the approximate groundwater flow direction and speed. There was little head difference between BH3 and BH4, but a difference of 0.08 m between BH4 and BH5. Using typical values for hydraulic conductivity $K \sim 3\times10^{-4}$ m/s and porosity $n \sim 0.3$ of sands and gravels (Domenico and Schwartz, 1998) gave an estimated seepage velocity of $v \sim 0.5$ m/day between BH4 and BH5.

A strong saline tracer (1000 litres, at a concentration of 40 g/l) was introduced into the minor aquifer via BH4 to provide a high resistivity contrast. Density driven flow was assumed to be insignificant due to the underlying aquiclude. Resistivity monitoring data were collected every four hours, and inverted to reveal the spatial distribution of the tracer in 3D (Figure 4). The images are displayed normalised to a baseline image obtained prior to injection, so conductive regions are shown as resistivity ratios < 1. They indicate that the tracer is predominantly localised in a horizontal aquifer that is reasonably uniform, and approximately 1 m thick, throughout the model space. The absence of conductivity increases above 5 m bgl implies that there is little upwards migration of tracer through fissures in the clay, and that the aquifer is reasonably well confined. There is some evidence that at $t = 0$ a fraction of the

tracer escaped from the injection point, suggesting that either the base or the sides of BH4 are not perfectly sealed. By contrast there appear to be no losses from the electrode array boreholes, which helps confirm that no pollution pathways were created during the array installations. The tracer speed can be estimated directly from the models by finding the times of minimum resistivity at discrete points throughout the model. This process gives an average $v = 0.49 \pm 0.07$ m/day, in excellent agreement with the value derived from the estimated material parameters. This result therefore provides confidence that geoelectrical monitoring has accurately mapped the dispersal of the tracer.

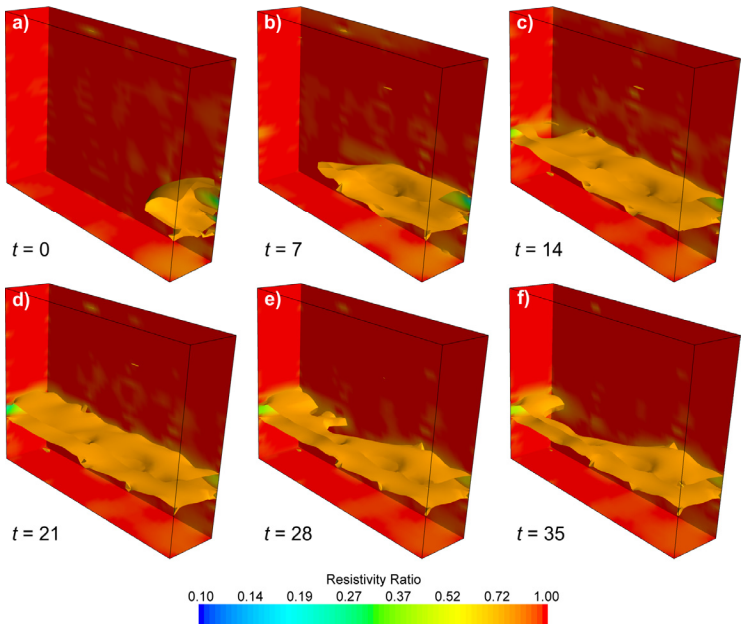

Figure 4. Evolution of the conductive tracer visualised in 3D at discrete times t (days). The isosurface ratio = 0.79.

Conclusion

The tracer test in particular has demonstrated that automated geoelectrical imaging can track and monitor, at field-scale in near real-time, contaminants that affect the electrical resistivity of the subsurface. By enabling the direct observation of dispersion and dilution processes, the test has shown that geoelectrical monitoring of remediation is directly applicable to situations where monitored natural attenuation is appropriate. However, there is no reason why the concept should not be equally applicable to most other in-situ remediation techniques operating on similar time-scales (i.e. a few hours or more).

Acknowledgements

This paper is published with the permission of the Executive Director of the British Geological Survey (NERC). The research was part of the CL:ARET (Contaminated Land: Assessment of Remediation by Electrical Tomography) project, which was funded by a grant from the Technology Strategy Board (www.innovateuk.org; project TP/5/CON/6/I/H0048B) and contributions from a consortium partnership comprising VHE Construction PLC, the British Geological Survey, Interkonsult Ltd and South Kesteven District Council.

References

Arps, J. J. [1953] The effect of temperature on the density and electrical resistivity of sodium chloride solutions. Petroleum Transactions AIME 198, 327-330.

Domenico, P. A. and Schwartz, F. W. [1998] Physical and Chemical Hydrogeology. (New York: John Wiley & Sons.) ISBN 0 471 59762 7

Oldenborger, G. A., Partha, S. R. and Knoll, M. D. [2007] Model reliability for 3D electrical resistivity tomography: Application of the volume of investigation index to a time-lapse monitoring experiment. Geophysics 72, F167-F175.

Wilkinson, P. B., Chambers, J. E., Lelliot, M., Wealthall, G. P. and Ogilvy, R.D., [2008] Extreme sensitivity of crosshole electrical resistivity tomography measurements to geometric errors. Geophysical Journal International 173, 49-62.